Establishing a Mechanical Homeostatic State in the Cardiac System to Study Growth and Remodeling of the Myocardial Tissue

Teresa Díaz Jordá[1], Martin R Pfaller[2], Marcos Latorre[1], Shaiv Parikh[1]

[1] Center for Research and Innovation in Bioengineering, Universitat Politècnica de València, Spain
[2] Department of Biomedical Engineering, Yale University, New Haven, USA

Abstract

Initializing growth and remodeling (G&R) simulations requires defining a stress-free configuration of the tissue from an in vivo, mechanobiologically equilibrated state. This is complex in Constrained Mixture Models (CMMs), where tissue is a mixture of constituents, each requiring a unique natural, stress-free state. When assembled and pre-stretched, these constituents must form a composite tissue in mechanical equilibrium. In our framework, the pre-stretches of collagen and muscle cells are prescribed, while the natural configuration of elastin remains unknown. Existing methods to solve this inverse problem are often cumbersome, as they require intrusive modifications to the computational solver. We provide a simplified two-stage approach: first, we establish whole-tissue mechanical equilibrium and subtract the stress contribution from the prescribed collagen and muscle, thereby isolating the stress state experienced by the elastin network. Second, an iterative algorithm determines elastin's stress-free state by running forward finite element simulations and updating the guessed configuration until the simulated deformation matches the in vivo geometry. We verified our method against an analytical solution in a cylindrical geometry. Consequently, we demonstrated its applicability in an idealized left ventricle model, enabling future mechanistic cardiac G&R studies.

1. Introduction

Growth and remodeling (G&R) in soft tissues can be triggered by a loading perturbation of its preferred, mechanical homeostatic state [1]. Constrained mixture models (CMMs) are a mathematical framework in which the G&R of soft tissues is modelled as the evolution of a composite material where structurally significant constituents, such as elastin, collagen and muscle cells, each with their own stress-free state, are constrained to a common loaded configuration, while mechanical equilibrium is maintained at the tissue-level. [2]. CMMs use the loaded *in vivo* state as the reference configuration [1], which requires determining a deposition stretch for each constituent. Deposition stretch or a pre-stretch is the stretch from a constituent's stress-free state to the tissue's *in vivo* configuration. The pre-stresses resulting from pre-stretches govern the tissue's mechanical homeostasis and simultaneously ensure mechanical equilibrium. Pre-stretch values for collagen and muscle cells are commonly prescribed based on ex vivo experimental data from vascular tissue [3]. However, quantifying elastin's pre-stretch remains a challenging problem. Computational inverse methods have been previously applied to estimate the stress-free reference configuration at tissue-level [4,5] as well as specifically for elastin [6]. These methods can be broadly categorized by their fundamental approach. For instance, the Backward Incremental Method (BIM) [5] operates entirely on the *in vivo* geometry. It calculates pre-stresses by incrementally loading the tissue and assigning the resulting incremental stresses back onto the loaded in vivo configuration; it does not explicitly estimate a unique stress-free geometry. In contrast, reverse-forward methods like the Augmented Iterative Method (AIM) [4] directly solve for the stress-free (zero-pressure) configuration. The algorithm iteratively refines an estimate of this stress-free state. On each iteration, it runs a standard forward simulation to load this guessed configuration, stopping only when the simulated deformed state matches the true in vivo geometry. The former approach is cumbersome as it demands modifications to the numerical solver to formulate the inverse problem, such as applying the stresses from the forward deformations applied to the *in vivo* configuration. In contrast, latter methods can leverage standard finite element solvers in a straightforward manner, without fundamental alterations to their core code. Our goal is to develop a forward method to determine the stress-free configuration of elastin that will allow initialization of CMMs G&R simulations, ensuring mechanical homeostasis. We have implemented and tested this method using two geometries: a straight cylindrical vessel and an idealized ventricle.

2. Methods

We introduced a two-staged computational framework to numerically estimate the stress-free configuration of elastin (Figure 1). This computational pipeline was implemented using GIBBON MATLAB library [7] and the finite element (FE) solver FEBio [8].

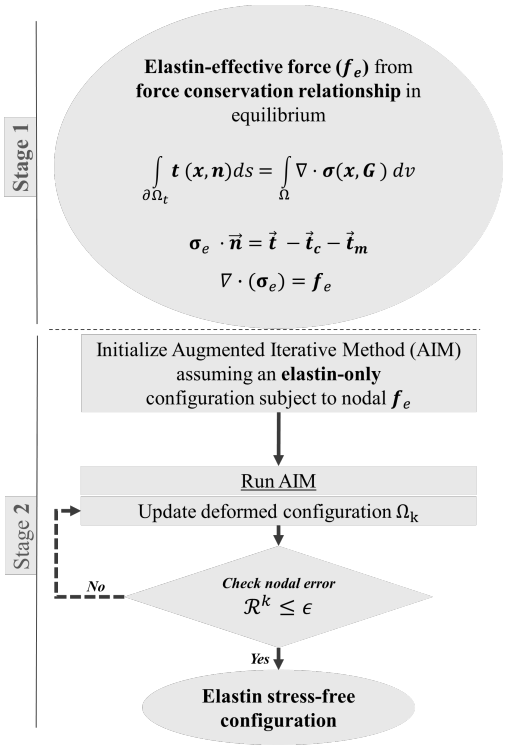

Figure 1. Flowchart for the two-stage implementation. Stage 1: elastin effective forces are computed. Stage 2: AIM is run to find the stress-free configuration of elastin. *ds*: surface element ($\in \Omega_t$); *dv*: volume element ($\in \Omega$).

2.1. Stage 1: Force balance in equilibrium

In this stage, we determine the stress experienced by the elastin network under conditions of mechanobiological equilibrium. We assume that in the current deformed configuration of a biological organ (Ω), with position of every point represented by $\boldsymbol{x}$, is subjected to traction ($\vec{\boldsymbol{t}}$) on boundary $\partial\Omega_t$. The traction forces result from the pressure (P_{ivo}) applied at the boundary of the tissue.

$$\vec{\boldsymbol{t}} = P_{ivo} \cdot \vec{\boldsymbol{n}} \tag{1}$$

where $\vec{\boldsymbol{n}}$ is a normal vector to the boundary (e.g., the arterial lumen or ventricular endocardium).

In CMMs, the total stress accounts for the weighted sum of the stresses carried by each of its individual constituents. The balance of linear momentum at $\forall \boldsymbol{x}$ yields the condition $\nabla \cdot (\phi_e \boldsymbol{\sigma}_e(\boldsymbol{G}_e) + \phi_c \boldsymbol{\sigma}_c(\boldsymbol{G}_c) + \phi_m \boldsymbol{\sigma}_m(\boldsymbol{G}_m)) = \boldsymbol{0}$, where $\nabla\cdot$ represents divergence operator, which gives the net internal force arising tissue stresses, ϕ_i are homeostatic constituent mass fractions and $\boldsymbol{\sigma_i}$ are the Cauchy stresses of the load-bearing constituents ($i =$ elastin (e), collagen (c) and muscle cells (m)) that arise from the deposition stretch tensors $\boldsymbol{G}_i = \partial \boldsymbol{x}/\partial \boldsymbol{X}_i$. $\boldsymbol{X}_\alpha (\in \Omega_{0,\alpha})$ represents the natural configuration of the constituent. For fibrous constituents such as collagen and muscle cells, we prescribe known homeostatic stretches λ_h^i and fiber directions $\boldsymbol{a}_0^i$ and the deposition stretch tensor as

$$\boldsymbol{G}_i = \lambda_h^i \boldsymbol{a}_0^i \otimes \boldsymbol{a}_0^i + \frac{1}{\sqrt{\lambda_h^i}} \left(\boldsymbol{I} - \boldsymbol{a}_0^i \otimes \boldsymbol{a}_0^i\right). \tag{2}$$

Cauchy stresses $\boldsymbol{\sigma}_c$ and $\boldsymbol{\sigma}_m$ can thus be calculated and translated to forces as $\nabla \cdot (\boldsymbol{\sigma}_c + \boldsymbol{\sigma}_m) = \boldsymbol{f}_c + \boldsymbol{f}_m$. For $\boldsymbol{x} \in \partial\Omega_t$ in mechanical equilibrium, the internal forces must balance the traction forces on the boundary $\boldsymbol{\sigma} \cdot \vec{\boldsymbol{n}} = \vec{\boldsymbol{t}}$, and as we isolate the unknown stresses of elastin for $\boldsymbol{x} \in \partial\Omega_t$ we obtain

$$(\boldsymbol{\sigma}_e + \boldsymbol{\sigma}_c + \boldsymbol{\sigma}_m) \cdot \vec{\boldsymbol{n}} = \vec{\boldsymbol{t}} \Rightarrow \boldsymbol{\sigma}_e \cdot \vec{\boldsymbol{n}} = \vec{\boldsymbol{t}} - \vec{\boldsymbol{t}}_c - \vec{\boldsymbol{t}}_m \tag{3}$$

Thus, satisfying this relationship (Eq.3) and the traction boundary condition (Eq. 1), we obtain the net nodal forces that are experienced by elastin as $\boldsymbol{f}_e = \boldsymbol{\sigma}_e \cdot \vec{\boldsymbol{n}}$.

2.2. Stage 2: Prestressing algorithm

To determine the natural stress-free configuration of elastin Ω_0^e and ultimately determine elastin pre-stretches, we coupled our approach with the Augmented Iterative Method (AIM), previously described in a previous study [4]. Briefly, the principle of this algorithm is to find a reference configuration (stress-free, Ω_0^e) so that, when subject to forces provided ($\boldsymbol{f}_e$), it deforms to Ω_{ivo}. The AIM iteratively updates a reference configuration Ω_0^{k+1} by subtracting the per node displacement vector ($\boldsymbol{\mathcal{R}^k} = \boldsymbol{x}^k - \boldsymbol{x}^*, \boldsymbol{x}^* \in \Omega_{ivo}$) between the updated deformed configuration Ω_k and the *in vivo* configuration, which is captured by a residual $\mathcal{R}^k = \|\boldsymbol{R}^k\|$. The algorithm stops when the residual falls below a defined tolerance ϵ ($= 10^{-3}$). Thus, iteratively running forward finite element FE simulation $\boldsymbol{\mathcal{S}}$ expressed in Equation 4, providing net nodal forces $\boldsymbol{f}_e$ we can obtain $\boldsymbol{X}_e^k$ as the nodal coordinates for the stress-free elastin configuration Ω_0^e:

$$\boldsymbol{x}^k = \boldsymbol{\mathcal{S}}\left(\left(\boldsymbol{X}_e^k, \boldsymbol{0}\right), \boldsymbol{f}_e\right) \tag{4}$$

2.3. Numerical verification

A cylindrical geometry was considered to verify the prestressing algorithm against an analytical solution of a stress-free configuration of elastin. We model an arterial segment as a cylinder (length l = 2.50 mm, inner diameter $r_i = 0.647$ mm, wall thickness $h = 0.04$ mm) discretized into 1860 linear hexahedral elements. The tissue is considered as a composite of elastin and collagen so that the stress contribution of each is weighted by its mass fraction ϕ_i (i = elastin, collagen). Collagen homeostatic

pre-stretch $\lambda_h^c = 1.10$ and a pressure of $P_{ivo} = 13.98$ kPa were prescribed. Only circumferential fibers were considered for simplification of the analytical problem. Collagen is modeled as in [1] with energy strain function

$$\Psi_c = \frac{c_1}{4c_2}\left(\exp(c_2(\mathbf{C}\,(\mathbf{G_c}):\vec{\boldsymbol{a}}\otimes\vec{\boldsymbol{a}} - 1)^2) - 1\right) \qquad (5)$$

Where **C** is the right Cauchy-Green deformation tensor, $\vec{\boldsymbol{a}}$ is the mean fiber direction and stiffness-like and non-dimensional stiffening parameters $c_1^c = 235$ kPa and $c_2^c = 4.08$ kPa, respectively. Mass fraction $\phi_c = 0.33$, and the amorphous elastin matrix is modeled as a neo-Hookean material by means of a simplified hyperelastic Ogden strain energy function

$$\Psi_e = \sum_{i=1}^{N} \frac{c_i}{m_i^2}(\tilde{\lambda}_1^{m_i} + \tilde{\lambda}_2^{m_i} + \tilde{\lambda}_3^{m_i} - 3) + \frac{K}{2}(J-1)^2 \qquad (6)$$

with $c_1^e = 1600$ kPa, $c_2^e = 0$, $K = 4160$ kPa, $m_1 = 2$ and mass fraction $\phi_e = 0.67$. We apply Dirichlet boundary conditions to constrain the displacement in the axial directions ($\boldsymbol{u}\,(\boldsymbol{x})_{\boldsymbol{z}} = \mathbf{0}$) on one end of the cylinder.

To validate our numerical approach, we derived an analytical solution for a thin-walled cylindrical tube under internal pressure. For such a geometry, the circumferential stress is given by $\sigma^\theta = P \cdot r_i/h$, where P is the internal pressure, r_i is the internal radius, and h is the wall thickness of the loaded *in vivo* geometry. By applying this stress-strain relationship within the constitutive model for the tissue, we solved for the unloaded geometry. This provided the ground truth values for the internal radius R_i^{GT} and wall thickness H_i^{GT} of the stress-free configuration, which we verified against the same parameters on the numerical solution.

2.4. Left ventricle prestressing

We considered an idealized left ventricle (LV) mesh represented as a truncated ellipsoid (major epicardial radius $a_{epi} = 20$mm minor epicardial radius $b_{epi} = 10$mm, and uniform wall thickness $h = 3$mm) discretized into 900 linear hexahedral elements. We modeled both collagen and cardiomyocyte fibers as hyperelastic materials with a preferred fiber orientation as in Eq. 5. Collagen follows the four-fiber family material model, which includes the contribution of circumferential, axial and two diagonal (±45º) fiber directions [1] and material parameters $c_1^c = 234.9$ kPa, $c_2^c = 4.08$. Cardiomyocyte fibers follow a helix angle that varies continuously from +60º at the endocardium to −60º at the epicardium, following energy strain as in Eq.5, and its material parameters $c_1^m = 261.4$ kPa, $c_2^m = 0.24$. Similarly to the cylinder case, elastin is modeled as in Eq.6 with $c_1^e = 89.71$ kPa, $c_2^e = 0$, $k_e = 89.71 \cdot 10^3$ kPa, $m_1 = 2$. Constituent mass fractions are equally distributed $\phi_e = \phi_c = \phi_m$. The fiber pre-stretches prescribed were $\lambda_h^c = 1.062$, and $\lambda_h^m = 1.10$. Material parameters were taken from vascular G&R model [1] and pre-stretches from [6] from vascular tissue as well. A pressure of 16 kPa (=120 mmHg) was prescribed on the endocardium boundary. The AIM was run with Dirichlet conditions on the nodes in the base in axial and circumferential directions ($\boldsymbol{u}\,(\boldsymbol{x})_{\boldsymbol{\theta}} = \mathbf{0}$, $\boldsymbol{u}\,(\boldsymbol{x})_{\boldsymbol{z}} = \mathbf{0}$; $\boldsymbol{x} \in \partial\Omega_{base}$).

3. Results and discussion

3.1. Cylinder case – Analytical solution

We assessed the agreement between our method and the analytical solution. We assessed the agreement between our method and the analytical solution. Using the forces ($\boldsymbol{f}_e$) from Stage 1, we compared our numerical solution for the inner radius (R_i) and thickness (H_i) in the unloaded configuration against the theoretical values derived from the analytical model for thin-walled cylinders. Numerically, we obtain that $R_i = 5.90 \cdot 10^{-1}$ mm and $H_i = 4.16 \cdot 10^{-2}$ mm, while the analytical ground truth values are $R_i^{GT} = 5.90 \cdot 10^{-1}$mm and $H_i^{GT} = 4.17 \cdot 10^{-2}$mm, showing a match for the inner radius and a small error (0.24%) for the thickness. The AIM reached a minimum nodal error $\mathcal{R}^k = 7.50 \cdot 10^{-4}$ mm (tolerance $\epsilon = 10^{-3}$mm) in 5 iterations. The agreement between our numerical result and the analytical solution shows the accuracy of the AIM implementation in solving the mechanobiological equilibrium problem.

3.2. Left ventricle prestress

We ran our algorithm on an idealized LV. In Figure 2, the unstressed configuration of elastin obtained with AIM is shown.

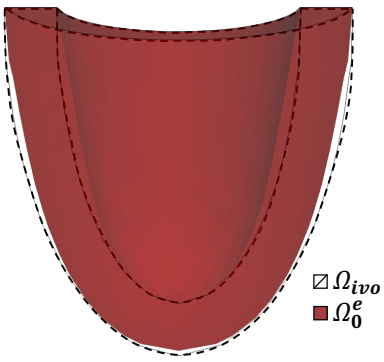

Figure 2. Cut view of the stress-free configuration of elastin (red) and in vivo LV geometry (dotted) obtained with the AIM implementation.

The convergence of the AIM is shown in Figure 3. After 8 iterations, a minimum residual $\mathcal{R}^k = 4 \cdot 10^{-4}$ mm was achieved, which is the minimum nodal difference between the original *in vivo* configuration and the updated *in vivo* geometry. By defining elastin's baseline mechanical state, our approach provides the reference needed to study maladaptive G&R.

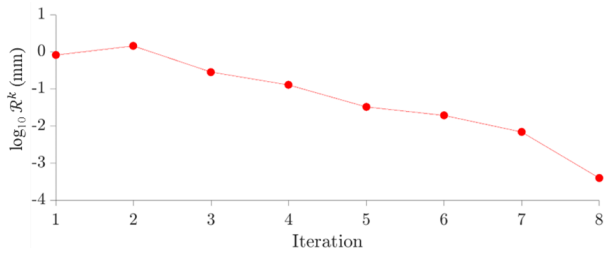

Figure 3. Augmented Iterative Method (AIM) convergence upon achieving minimum nodal error $\boldsymbol{\mathcal{R}^k \leq \epsilon}$ for $\boldsymbol{\epsilon = 10^{-3}}$mm.

4. Limitations and future perspectives

This study has several limitations that provide a clear pathway for future research. Firstly, it is worth noting that the material parameters used were taken from the vascular G&R model developed in [1], while collagen and cardiomyocyte homeostatic pre-stretches were adopted from [6], which were also derived from vascular tissue, since CMM parameters for myocardium have not yet been characterized. Hence, the presented results cannot be considered physiologically relevant but rather a proof of concept of a forward method. Secondly, the imposed Dirichlet boundary conditions on the base of the ventricle, while necessary for numerical stability, introduce artificial constraints that prevent a perfectly satisfied global force balance, potentially influencing the local stress field in the elements at the base. Employing alternative conditions like Robin-type boundaries (applying a compliant constraint that balances force with displacement) in future studies could mitigate this issue [6]. Additionally, comprehensive benchmarking against other established pre-stress algorithms using a wider range of material models will be essential for rigorously verifying the method's robustness and performance. Finally, to fully establish this framework, future work will focus on applying the algorithm to realistic, patient-specific geometries derived from medical imaging.

5. Conclusions

By applying continuum mechanics principles, the developed framework infers the constituent-specific homeostatic forces that define mechanical equilibrium. The coupling of this principle with a forward iterative approach such as the AIM provides a robust methodology to estimate the initial state of elastin in mechanobiological equilibrium. We have tested our algorithm by comparing our numerical solution with the known analytical solution for a thin-walled cylinder, showing agreement between them. Unlike backward methods that require complex implementations within the solver, the presented method should be easy to implement in any FE solver as it only relies on iterative forward simulations until convergence is achieved. While we have demonstrated its effectiveness on idealized cardiovascular models - vessel and a left ventricle- our methodology is a general approach applicable to any 3D geometry to enable the study of CMM G&R in a wide range of soft tissues.

Acknowledgments

This work was supported by the European Union "Horizon Europe" research and innovation program (Grant Agreement 101039349 project G-CYBERHEART) and NIH R00HL161313.

References

[1] Latorre M, Humphrey JD. Fast, rate-independent, finite element implementation of a 3D constrained mixture model of soft tissue growth and remodeling. Computer Methods in Applied Mechanics and Engineering. 2020 Aug 15;368.

[2] Humphrey JD, Rajagopal KR. A Constrained Mixture Model for growth and remodeling of soft tissues. Math Model Methods Appl Sci. 2002 Mar 1;12(03):407–30.

[3] Cardamone L, Valentín A, Eberth JF, Humphrey JD. Origin of axial pre-stretch and residual stress in arteries. Biomechanics and Modeling in Mechanobiology. 2009;8(6):431–46.

[4] Rausch MK, Genet M, Humphrey JD. An augmented iterative method for identifying a stress-free reference configuration in image-based biomechanical modeling. Journal of Biomechanics. 2017 Jun 14;58:227–31.

[5] Tziotziou A, Liu Y, Fontana F, Bierens J, Nederkoorn PJ, de Jong PA, et al. Pressure- and flow-driven biomechanical factors associate with carotid atherosclerosis assessed by computed tomography angiography. Atherosclerosis. 2025;

[6] Gebauer AM, Pfaller MR, Braeu FA, Cyron CJ, Wall WA. A homogenized constrained mixture model of cardiac growth and remodeling: analyzing mechanobiological stability and reversal. Biomechanics and Modeling in Mechanobiology. 2023 Dec 1;22(6):1983–2002.

[7] Moerman KM. GIBBON: The Geometry and Image-Based Bioengineering add-On. The Journal of Open-Source Software. 2018 Feb 19;3(22):506.

[8] Maas SA, Ellis BJ, Ateshian GA, Weiss JA. FEBio: Finite Elements for Biomechanics. Journal of Biomechanical Engineering. 2012 Feb 9;134(1).

Address for correspondence:

Shaiv Parikh
Centro de Investigación e Innovación en Bioingeniería (Ci2B), Universitat Politècnica de València (UPV), Valencia, Spain.
saparik1@upvnet.upv.es